Available online at www.sciencedirect.com
ScienceDirect
Physics of the Earth and Planetary Interiors 170 (2008) 248–259
PHYSICS OF THE EARTH AND PLANETARY INTERIORS
www.elsevier.com/locate/pepi

Spin transition of iron in the Earth's lower mantle

Jung-Fu Lin [a,*], Taku Tsuchiya [b]

[a] Lawrence Livermore National Laboratory, 7000 East Avenue, Livermore, CA 94550, USA
[b] Geodynamics Research Center, Ehime University, 2-5 Bunkyo-cho, Matsuyama 790-8577, Japan

Received 22 June 2007; received in revised form 27 November 2007; accepted 15 January 2008

Abstract

Electronic spin-pairing transitions of iron and associated effects on the physical properties of host phases have been reported in lower-mantle minerals including ferropericlase, silicate perovskite, and possibly in post-perovskite at lower-mantle pressures. Here we evaluate current understanding of the spin and valence states of iron in the lower-mantle phases, emphasizing the effects of the spin transitions on the density, sound velocities, chemical behavior, and transport properties of the lower-mantle phases. The spin transition of iron in ferropericlase occurs at approximately 50 GPa and room temperature but turns into a wide spin crossover under lower-mantle temperatures. Current experimental results indicate a continuous nature of the spin crossover in silicate perovskite at high pressures, but which valence state of iron undergoes the spin crossover and what is its associated crystallographic site remain uncertain. The spin transition of iron results in enhanced density, incompressibility, and sound velocities, and reduced radiative thermal conductivity and electrical conductivity in the low-spin ferropericlase, which should be considered in future geophysical and geodynamic modeling of the Earth's lower mantle. In addition, a reduction in sound velocities within the spin transition is recently reported. Our evaluation of the experimental and theoretical pressure–volume results shows that the spin crossover of iron results in a density increase of 2–4% in ferropericlase containing 17–20% FeO. Here we have modeled the density and bulk modulus profiles of ferropericlase across the spin crossover under lower-mantle pressure–temperature conditions and shown how the ratio of the spin states of iron affects our understanding of the state of the Earth's lower mantle.

Keywords: Spin transition; Lower mantle; Mineral physics; Ferropericlase; Silicate perovskite

1. Introduction

Earth's lower mantle is the most voluminous layer of the Earth and consists of ~33% ferropericlase [(Mg,Fe)O] and ~62% aluminous silicate perovskite [Al–(Mg,Fe)SiO_3], together with ~5% calcium silicate perovskite ($CaSiO_3$), based on a pyrolitic compositional model (Ringwood, 1982). Recent studies also show that silicate perovskite transforms to a post-perovskite structure just above the core–mantle region, the D″ layer (e.g., Murakami et al., 2004; Oganov and Ono, 2004; Tsuchiya et al., 2004). Although the Earth's lower mantle was thought to be relatively pristine seismically and geochemically compared to the transition zone and the D″ layer, a range of geophysical evidence indicates that seismic and geochemical heterogeneities exist in the mid-lower mantle (e.g., Dziewonski and Anderson, 1981; Kellogg et al., 1999; van der Hilst and Kárason, 1999; Trampert et al., 2004). It was thought for decades that of particular importance to such heterogeneities are the variation of iron content in host minerals and temperature fluctuation in the lower mantle. The surprising discovery of the electronic high-spin (HS) to low-spin (LS) transition (spin-pairing transition) of iron in the lower-mantle phases and its associated effects, however, challenges this classical view and shows that the Earth's interior is more complex than previously thought (e.g., Lin et al., 2007a).

The enormous nuclear binding energy of iron gives rise to its universal natural abundance, and as such, iron (Fe) is the most abundant 3d transition metal in the Earth's interior. Although the exact composition of the lower mantle has yet to be unambiguously determined (Mattern et al., 2005), current consensus for its iron abundance and valence states is that iron exists mainly in ferrous iron (Fe^{2+}) with a concentration level of approximately 20% in ferropericlase, whereas iron exhibits two main valence states, Fe^{2+} and ferric iron (Fe^{3+}), with a total concentration level of approximately 10% in silicate perovskite. The ferric iron content in silicate perovskite strongly correlates with the concentration of Al (McCammon, 1997).

* Corresponding author. Tel.: +1 925 424 415; fax: +1 925 422 6594.
E-mail address: afu@llnl.gov (J.-F. Lin).

0031-9201/$ – see front matter © 2008 Elsevier B.V. All rights reserved.
doi:10.1016/j.pepi.2008.01.005

Because of the partially filled 3d-electron orbitals, the electronic valence and spin states of iron in its host phases have been reported to vary under lower-mantle conditions. Of particular importance to the geophysics and geochemistry of the lower mantle are the associated physical and chemical properties of the valence and spin states of iron in the lower mantle minerals (e.g., Burns, 1993; McCammon, 2006). In particular, electronic spin-pairing transitions of iron that were proposed decades ago (e.g., Fyfe, 1960; Gaffney and Anderson, 1973; Ohnishi, 1978; Sherman, 1988, 1991; Sherman and Jansen, 1995) have been recently detected in the lower-mantle minerals including ferropericlase, silicate perovskite, and possibly in post-perovskite at high pressures (e.g., see Lin et al., 2007a for a brief summary). Here we evaluate the nature of the spin transition and its associated effects on the physical properties of the deep-mantle phases such as the density, sound velocities, chemical behavior, and transport properties. Because the effects of the spin transitions on the density and incompressibility of ferropericlase have been relatively well studied theoretically and experimentally, we have calculated the density and bulk modulus profiles of ferropericlase across the spin crossover at high pressures and temperatures. These new results provide further insights into the nature of the spin transition and its consequences in the state of the lower mantle.

2. Electronic spin transition of iron in the lower-mantle minerals

The 3d electrons of iron can occupy differently degenerate sets of 3d orbitals, namely the triplet t_{2g}-like and doublet e_g-like orbitals in the case of the sixfold, octahedrally coordinated iron in ferropericlase. The occupation of the 3d orbitals is defined by the surrounding environment of the iron atom which is influenced by factors such as the bond length, crystallographic site, pressure, and temperature (some of these parameters can be interconnected). Under ambient conditions in silicates and oxides, it is energetically favorable for the 3d electrons to occupy different orbitals with the same electronic spin, that is, the high-spin state with four unpaired electrons and two paired electrons in Fe^{2+} (spin quantum number (S) = 2), for example. In this case, the hybridized t_{2g}-like and e_g-like orbitals of the sixfold coordinated iron are separated by the crystal-field splitting energy (Δ), which is lower than the electronic spin-pairing energy (Λ). The crystal-field splitting energy with respect to the spin-pairing energy, however, can be significantly influenced by the energy change associated with pressure, temperature, and/or composition. The increase of the crystal-field splitting energy with respect to the spin-pairing energy under high pressures can eventually lead to the pairing of the 3d electrons of the opposite spin, that is, the low-spin state with all six 3d electrons paired in Fe^{2+} (S = 0). The scheme of the crystal-field splitting energy relative to the spin-pairing energy, however, becomes rather complex through crystallographic site distortion and electronic band overlap where occupancy degeneracy may be lifted (e.g., Burns, 1993) such as in silicate perovskite and post-perovskite, making modeling of the experimental data and theoretical treatment of the spin transition rather complicate (e.g., Tsuchiya et al., 2006a,b). In particular, the degeneracy of the electronic energy levels can be lifted through Jahn–Teller effect.

2.1. Electronic spin transition of iron in ferropericlase

Pressure-induced isosymmetric spin-pairing transitions of iron in ferropericlase have been reported using X-ray emission spectroscopy (Badro et al., 2003; Lin et al., 2005, 2006a, 2007b,d), conventional and synchrotron Mössbauer spec-

Table 1
List of experimental and theoretical studies on the spin transition of iron in ferropericlase at high pressures

Composition	Method	Transition pressure (GPa)	Reference
$(Mg_{0.83},Fe_{0.17})O$	X-ray emission	Approximately 60–70	Badro et al. (2003)[a]
$(Mg_{0.75},Fe_{0.25})O$	X-ray emission	54–67	Lin et al. (2005)[b] and Vankó and de Groot (2007)[c]
$(Mg_{0.60},Fe_{0.40})O$	X-ray emission	84–102	Lin et al. (2005)[b]
$(Mg_{0.75},Fe_{0.25})O$	Synchrotron Mössbauer	52–70	Lin et al. (2006a)
$(Mg_{0.95},Fe_{0.05})O$	X-ray emission	46–55	Lin et al. (2006a, 2007b)[c]
$(Mg_{0.80},Fe_{0.20})O$	Conventional Mössbauer	55–105	Kantor et al. (2006)
$(Mg_{0.80},Fe_{0.20})O$	Conventional Mössbauer	40–60	Speziale et al. (2005)
$(Mg_{0.83},Fe_{0.17})O$	Theory	65 (assumed)	Sturhahn et al. (2005)[d]
$(Mg_{0.8125},Fe_{0.1875})O$	Theory	32 (±2)	Tsuchiya et al. (2006a)[e]
$(Mg_{0.75},Fe_{0.25})O$	Theory	69, 106	Persson et al. (2006)[f]
$(Mg_{0.75},Fe_{0.25})O$	Optical absorption	~55–65	Goncharov et al. (2006)[g]
$(Mg_{0.88},Fe_{0.12})O$	Optical absorption	51–60	Keppler et al. (2007)[h]

The Fe^{3+} content in most of these studies is negligible. Results for iron content of 50% or more are not listed for simplicity.

[a] Transition pressure was not well defined due to limited number of spectra.

[b] Transition pressure and spin states were derived from the integration of the intensity of the satellite Kβ' peak.

[c] Transition pressure and spin states were derived from the integrals of the absolute values of the difference spectra.

[d] Transition pressure at 65 GPa is assumed whereas spin crossover along geotherm is predicted based on crystal-field and extended Bragg–Williams mean-field theory.

[e] Based on first principles with internally consistent LDA + U at high pressures and 0 K and a spin crossover is predicted at high pressures and temperatures.

[f] Based on GGA + U, transition pressure is 69 GPa when U is 3 eV and 106 GPa when U is 5 eV.

[g] Based on absorption bands and edges; other compositions of $(Mg_{0.94},Fe_{0.06})O$ and $(Mg_{0.85},Fe_{0.15})O$ were also examined.

[h] If changes in the optical spectra are associated with the spin transition.

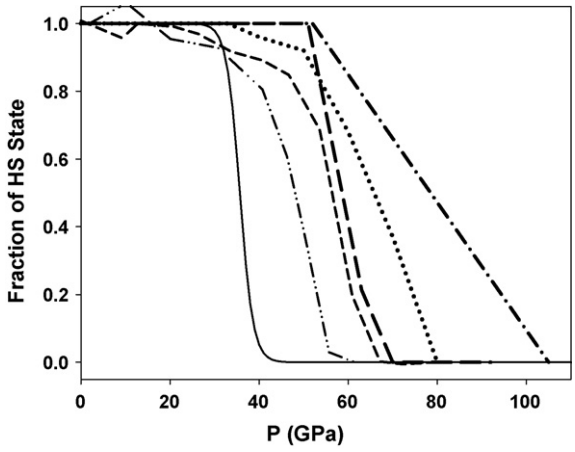

Fig. 1. Fraction of the high-spin iron relative to the low-spin iron in ferropericlase as determined from recent high-pressure Mössbauer and X-ray emission measurements and theoretical calculations. Long dashed line: synchrotron Mössbauer of $(Mg_{0.75},Fe_{0.25})O$ at high pressures and 300 K (Lin et al., 2006a); short dashed line: X-ray emission of $(Mg_{0.75},Fe_{0.25})O$ at high pressures and 300 K (Lin et al., 2005; Vankó and de Groot, 2007); dotted line: traditional Mössbauer of $(Mg_{0.80},Fe_{0.20})O$ at high pressures and 6 K (Speziale et al., 2005); dash–dot line: traditional Mössbauer of $(Mg_{0.80},Fe_{0.20})O$ at high pressures and 300 K (Kantor et al., 2006); dash–dot–dot line: X-ray emission of $(Mg_{0.95},Fe_{0.05})O$ at high pressures and 300 K (Lin et al., 2006a, 2007a,b,c,d,e); thin solid line: representative theoretical calculations for $(Mg_{0.8125},Fe_{0.1875})O$ (Tsuchiya et al., 2006a). Theoretical results by Persson et al. (2006) are not shown here for clarity of the comparison. Except results from theoretical calculations (Persson et al., 2006; Tsuchiya et al., 2006a), all experimental results show that the spin transition starts to occur at approximately 40–50 GPa, though the width of the transition varies depending on the experimental techniques and sample conditions.

troscopy (Speziale et al., 2005; Gavriliuk et al., 2006; Kantor et al., 2006, 2007; Lin et al., 2006a), X-ray diffraction (Fei et al., 2007; Lin et al., 2005; Speziale et al., 2005), optical absorption (Goncharov et al., 2006; Keppler et al., 2007), nuclear resonant inelastic X-ray scattering (Lin et al., 2006b), electrical conductivity (Lin et al., 2007c), impulsive stimulated light scattering (Crowhurst et al., 2008), and classical and novel theoretical calculations (Sturhahn et al., 2005; Persson et al., 2006; Tsuchiya et al., 2006a,b) (Table 1, Figs. 1–4). Comparison of the derived fractions of the high-spin and low-spin states shows that the spin transition of iron starts to occur at approximately 40–50 GPa and 300 K, though the exact width of the transition varies significantly and appears to depend on the techniques used to probe the transition (Gavriliuk et al., 2006; Kantor et al., 2006, 2007; Lin et al., 2005, 2006a,b, 2007b,d; Speziale et al., 2005; Vankó and de Groot, 2007) (Fig. 1, Table 1). Notably, the spin states of iron in lower-mantle ferropericlase have been measured up to 95 GPa and 2000 K with X-ray emission spectroscopy in a laser-heated diamond cell (Lin et al., 2007d). A gradual spin transition zone (STZ) of iron occurs over a pressure–temperature range extending from approximately 1000 km in depth and 1900 K to 2200 km and 2300 K in the lower mantle (Lin et al., 2007d).

Here we briefly describe the underlying physics behind these experimental techniques used to probe the spin transition in order to help explicate current experimental results. In synchrotron X-ray Kβ emission spectroscopy (XES), the presence of the satellite peak (Kβ′) arises from the 3p–3d electronic exchange

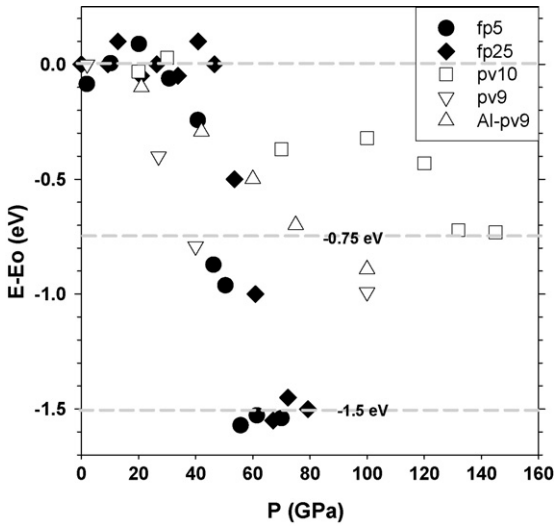

Fig. 2. Energy shift of the main Kβ emission peak of iron as a function of pressure for ferropericlase (solid symbols) and silicate perovskite (open symbols). Solid circles: $(Mg_{0.95},Fe_{0.05})O$ (Lin et al., 2007b); solid diamonds: $(Mg_{0.75},Fe_{0.25})O$ (Lin et al., 2005, 2007b); open squares: $(Mg_{0.9},Fe_{0.1})SiO_3$ (Badro et al., 2004); open triangles down: $(Mg_{0.91},Fe_{0.09})SiO_3$ (Li et al., 2004); open triangles up: $(Mg_{0.88},Fe_{0.09})(Si_{0.94},Al_{0.10})O_3$ (Li et al., 2004). An energy decrease of 1.5–1.6 eV in the Kβ main peak was observed in both $(Mg_{0.95},Fe_{0.05})O$ and $(Mg_{0.75},Fe_{0.25})O$ across the spin transition (Fig. 1) and no energy shift was observable away from the spin transition region (Lin et al., 2007b).

interaction and is characteristic of the high-spin state of iron whereas the absence of the satellite peak indicates the occurrence of the low-spin state (Fig. 3) (e.g., Badro et al., 2003; Lin et al., 2005). However, the intensity of the satellite peak is a complex function of many factors, from which the average spin

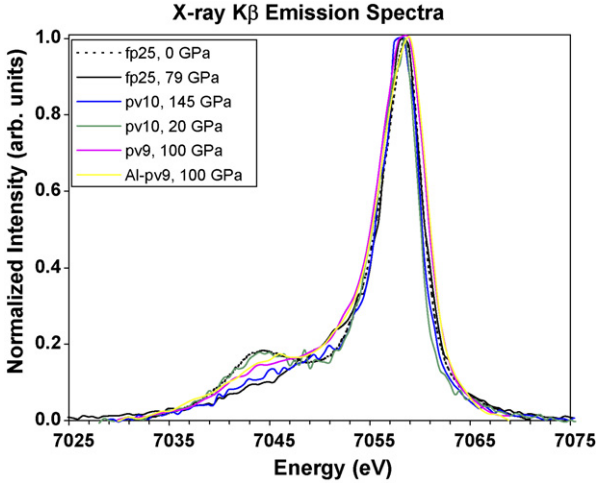

Fig. 3. Comparison of the X-ray emission spectra of ferropericlase and silicate perovskite under high pressures. The spectra are normalized to unity and shifted in energy to compensate for the pressure-induced shift of the line maximum based on the main fluorescence peak (Kβ) at 7058 eV. fp25 $(Mg_{0.75},Fe_{0.25})O$ at 0 GPa (high-spin state) and 79 GPa (low-spin state) (Lin et al., 2005). pv10 at 145 GPa: $(Mg_{0.9},Fe_{0.1})SiO_3$ (Badro et al., 2004); pv9 and Al-pv9 at 100 GPa: $(Mg_{0.91},Fe_{0.09})SiO_3$ and $(Mg_{0.88},Fe_{0.09})(Si_{0.94},Al_{0.10})O_3$, respectively (Li et al., 2004). The X-ray emission spectrum of the low-spin Fe_2O_3 (Badro et al., 2002) is very similar that of low-spin ferropericlase and is not shown for clarity.

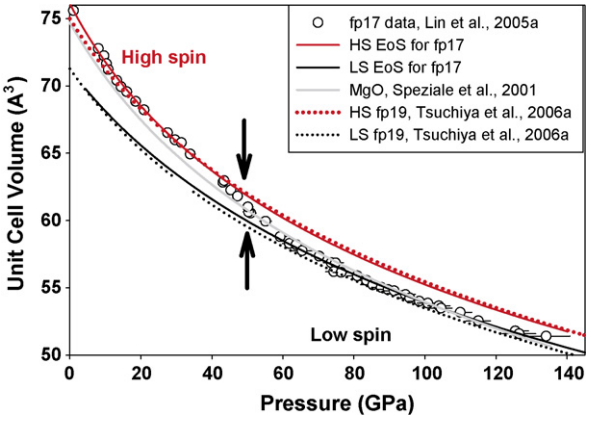

Fig. 4. Unit cell volume of ferropericlase across the spin transition. The low-spin ferropericlase has similar unit cell volume to that of MgO (gray line) but has higher incompressibility. The volume reduction across the spin transition at ~50 GPa, as indicated by vertical arrows, is 2.8% in X-ray diffraction (Fig. 5) (Lin et al., 2005) and 4.2% in theoretical calculations (Tsuchiya et al., 2006a). Open circles: X-ray diffraction data of $(Mg_{0.83},Fe_{0.17})O$ (Lin et al., 2005); gray line: MgO (Speziale et al., 2001); solid lines: equation of state fits to the experimentally determined data of the high-spin and low-spin ferropericlase, respectively (Lin et al., 2005); dotted lines: theoretically calculated equation of state of the high-spin and low-spin ferropericlase, respectively (Tsuchiya et al., 2006a). Here the K_{0T} for the high-spin state is 149.7 (±3.7) GPa with a K'_{0T} of 4.55 (±0.21), when fitted the experimental data up to 40 GPa. The K_{0T} for the low-spin ferropericlase is 205 (±16) GPa with V_{0LS}/V_{0HS} of 0.936 (±0.067) and an assumed K'_{0T} of 4, which is derived from fitting the experimental data above 61 GPa (Fig. 1).

number might be extracted when, for example, interpreted with the crystal-field theory (Badro et al., 2004, 2005; Li et al., 2004, 2006). To quantitatively derive the average spin number and the fraction of the high-spin and low-spin states, the integrated absolute difference (the IAD analysis) method is developed, which integrates the absolute values of the difference spectra and compares these integrals to that obtained on the references. Results show that the derived IAD values linearly correlate with the spin quantum number independently derived from Mössbauer experiments between two spin states and provide a reliable method for determining the fraction of the spin states in ferropericlase (Vankó et al., 2006; Vankó and de Groot, 2007; Lin et al., 2007b,d). These analyses generally agree with the integrated intensity of the satellite Kβ′ peak (Vankó and de Groot, 2007; Lin et al., 2007b,d). As an additional line of evidence for the electronic spin-pairing transition of iron, an energy decrease of 1.5–1.6 eV in the main Kβ peak was also observed in ferropericlase at pressures where the spin transition was detected by other methods (Fig. 2) (Lin et al., 2006a, 2007b,d), while no significant energy shift was observable at pressures away from the spin transition.

Conventional and synchrotron Mössbauer studies show that the quadrupole splitting (QS) disappears and the isomer shift (IS) drops significantly at approximately 50 GPa in ferropericlase, consistent with the high-spin to low-spin electronic transition of iron in the sample (Speziale et al., 2005; Gavriliuk et al., 2006; Kantor et al., 2006, 2007; Lin et al., 2006a); however, the reported width of the spin transition varies significantly from a narrow width in a synchrotron Mössbauer study (Lin et al., 2006a) to a very wide range in a conventional Mössbauer study (Kantor et al., 2006) (Table 1, Fig. 1). The discrepancy in these results may arise from different experimental conditions, such as the sample size, thickness, hydrostaticity in the sample chamber, and the beamsize of the X-ray source (Gavriliuk et al., 2006; Lin et al., 2007b). In particular, a very large sample and X-ray beamsize were used in traditional Mössbauer measurements (Kantor et al., 2006), likely resulting in a wide range of the spin transition. We note that X-ray emission and Mössbauer spectroscopies probe processes occurring in the inner electronic shell (in X-ray emission) or the nucleus of the iron atom (in Mössbauer) as indicators of the electronic spin transition which occurs in the outermost 3d orbitals of the iron atom.

Optical absorption spectroscopy has also been used to study the spin transition in ferropericlase, as the technique may directly probe the energy separation of the 3d orbitals involved in the transition (Goncharov et al., 2006; Keppler et al., 2007). The absorption spectra of ferropericlase, corresponding to the crystal-field bands, changes significantly between 50 and 65 GPa, consistent with the spin transition at high pressures. Other high-pressure techniques such as X-ray diffraction, nuclear resonant inelastic X-ray scattering spectroscopy, designer diamond anvil cell, and impulsive stimulated light scattering are also used to probe the associated effects of the spin transition on the volume, partial phonon density of states (PDOS), and electrical conductivity of ferropericlase (Lin et al., 2005, 2006b, 2007c; Speziale et al., 2005; Crowhurst et al., 2008). These results will be discussed in more details in Sections 3 and 4.

Classical and novel theoretical calculations also provide new insights into the nature of the spin transition in ferropericlase (Sturhahn et al., 2005; Persson et al., 2006; Tsuchiya et al., 2006a,b). In particular, recently developed formalism using local density approximation (LDA) with an internally consistent Hubbard energy (U) (Cococcioni and de Gironcoli, 2005) has enabled much more reliable first principles studies on electronic structures of the strongly correlated Fe–O bonding (Tsuchiya et al., 2006b). Here, the on-site Coulomb interaction between the 3d electrons, which is characterized by the Hubbard energy, is determined at each given volume and iron concentration based on an internally consistent method, while it is determined empirically in the usual LDA + U calculations (e.g., Persson et al., 2006). Most noticeably, recent theoretical predictions indicate that the electronic spin-pairing transition of iron in ferropericlase occurs over a very narrow range of pressure at room temperature but turns to a macroscopically isosymmetric spin crossover with an extended transition pressure of approximately 30–50 GPa at the lower-mantle temperatures (Sturhahn et al., 2005; Tsuchiya et al., 2006a); though, the experimentally observed width of the spin crossover in ferropericlase is much narrower than what was predicted by the existing theoretical models (Sturhahn et al., 2005; Tsuchiya et al., 2006a). The spin crossover arises from the condition where the thermal energy at high temperatures and pressures is sufficient to overcome the energy difference between the high-spin state and low-spin state. Such a spin crossover is also expected to be a general phenomenon occurring in silicate perovskite and perhaps in post-perovskite at high

pressures and temperatures. Theoretical results also show that the intermediate spin state with two unpaired electrons ($S = 1$) is likely unstable at the pressure–temperature conditions of the lower mantle (Tsuchiya et al., 2006a); however, the existence of the intermediate-spin iron in perovskite is recently proposed experimentally.

Classical concept of the Clausius–Clapeyron phase transition boundary which typically considers the entropy and volume differences between two different phases (Badro et al., 2005; Lin et al., 2005, 2006a,b; Hofmeister, 2006) cannot be simply applied to understand the occurrence of the spin crossover phenomenon at lower-mantle pressure–temperature conditions, because the spin crossover involves a mixture of the high-spin and low-spin states over an extended pressure–temperature range (Tsuchiya et al., 2006a). Since certain assumptions are needed to understand the magnetic and electronic contributions to the energy difference between relevant spin states in theoretical calculations of the spin crossover (Sturhahn et al., 2005; Tsuchiya et al., 2006a), the natural width of the spin crossover of iron in the lower-mantle phases remains to be investigated experimentally (Lin et al., 2007d).

2.2. Electronic spin states of iron in silicate perovskite and post-perovskite

Iron in perovskite and perhaps in post-perovskite exists in the ferrous and/or ferric states and can possibly occupy one of two crystallographic sites, the large dodecahedral site and the small octahedral site (McCammon, 1997, 2006). Although the exact site occupancy of ferrous and ferric iron between these two sites is poorly characterized under high pressures, recent studies indicate that Fe^{2+} mainly occupies the large dodecahedral site (the A site) whereas Fe^{3+} together with lesser amounts of Fe^{2+} occupies the smaller octahedral site (the B site) (McCammon, 1997).

Electronic spin-pairing transitions of Fe^{2+} and/or Fe^{3+} have also been reported to occur in iron-bearing silicate perovskite and perhaps in post-perovskite using X-ray emission spectroscopy (Badro et al., 2004, 2005; Li et al., 2004), synchrotron Mössbauer spectroscopy (Jackson et al., 2005; Li et al., 2006), and theoretical calculations (Cohen et al., 1997; Li et al., 2005; Zhang and Oganov, 2006; Stackhouse et al., 2006, 2007), though these transitions appear to be more complex than that in ferropericlase likely due to the low-symmetry oxygen ligand field in perovskite and post-perovskite. While X-ray emission studies suggest a two-step transition at ~70 GPa for Fe^{2+} and 120 GPa for Fe^{3+} in $(Mg_{0.9},Fe_{0.1})SiO_3$ (Badro et al., 2004, 2005) or a gradual transition for Fe^{2+} alone, or concurrently with Fe^{3+}, in Al-bearing and Al-free perovskite (Li et al., 2004, 2006), high-pressure synchrotron Mössbauer studies indicate a continuous transition of Fe^{3+} (instead of the dominant Fe^{2+}) based on the deviation of the derived isomer shifts of Fe^{3+} relative to Fe^{2+} (Jackson et al., 2005). On the other hand, theoretical calculations on silicate perovskite show that Fe^{2+} remains in the high-spin state under lower-mantle pressures and that Fe^{3+} in the Mg site undergoes the electronic spin transition in which the transition pressure is reported to increase with increasing Al content in silicate perovskite (Li et al., 2005; Zhang and Oganov, 2006; Stackhouse et al., 2007) (Table 2); however, concurrent reports show that Fe^{2+} undergoes a spin transition between 130–145 GPa (Stackhouse et al., 2007). The stability of the intermediate-spin state with two unpaired electrons ($S = 1$) remains to be further investigated experimentally (Li et al., 2004), although theoretical calculations show that it is likely unstable at the high pressures (Li et al., 2005; Zhang and Oganov, 2006; Stackhouse et al., 2007).

Pictures for the spin and valence states of the post-perovskite phase at the conditions of the D″ layer are least clear. Based on the high-pressure X-ray emission spectra and simple crystal-field theory, it was suggested that Fe^{2+} in the dodecahedral and octahedral sites and Fe^{3+} in the octahedral sites are all in the low-spin state in post-perovskite at 145 GPa; however, no direct structural identification of the sample in the post-perovskite phase has been provided in the study (Badro et al.,

Table 2
List of experimental and theoretical studies on the spin transition of iron in silicate perovskite at high pressures

Composition	Fe^{3+} (%)	Method	Results	Reference
$(Mg_{0.9},Fe_{0.1})SiO_3$	~25	Emission	Fe^{2+} at 70 GPa, Fe^{3+} at 120 GPa	Badro et al. (2004)[a]
$(Mg_{0.91},Fe_{0.09})SiO_3$	~25	Emission	Fe^{2+} or with Fe^{3+} gradually	Li et al. (2004)[b]
$(Mg_{0.9},Fe_{0.1})SiO_3$	37	Mössbauer	Fe^{3+} completed at 70 GPa	Jackson et al. (2005)[c]
$FeSiO_3$	0	Theory	Gradual crossover in B site	Cohen et al. (1997)[d]
$(Mg,Fe)(Si,Al)O_3$	100	Theory	Fe^{3+} from 97 to 126 GPa	Li et al. (2005)[e]
$(Mg_{0.88},Fe_{0.09})(Si_{0.94},Al_{0.10})O_3$	50–70	Mössbauer	Fe^{2+}, or with Fe^{3+}, at 20–120 GPa	Li et al. (2006)[f]
$Al–(Mg,Fe)SiO_3$	0, 100	Theory	Fe^{3+} in Mg site at ~76–134 GPa	Zhang and Oganov (2006)[g]
$(Mg,Fe)SiO_3$	0–50	Theory	Fe^{3+}: 60–160 GPa; Fe^{2+}: 130–145 GPa	Stackhouse et al. (2007)[h]

[a] Total Fe^{3+} content was estimated from the conditions of sample synthesis and total iron concentration in the sample.
[b] Incomplete spin crossover of Fe^{2+} or with Fe^{3+} up to the highest pressure of 100 GPa in the study.
[c] No evidence for spin transition of Fe^{2+}; spin crossover of Fe^{3+} from 0 to 70 GPa based on the isomer shifts of Fe^{3+} relative to Fe^{2+}.
[d] No spin transition is reported for the A site and the transition pressure for the B site is not specified.
[e] Ferric iron (6.25 mol%) and Al (6.25 mol%) substitute for Mg and Si, respectively.
[f] Incomplete spin crossover based on synchrotron Mössbauer and X-ray emission results from Li et al. (2004).
[g] Transition pressure increases from ~76 GPa in Al-free perovskite to ~134 GPa in Al-bearing perovskite; Fe^{2+} in the high-spin state and Fe^{3+} in Si site in the low-spin state at the mantle pressures.
[h] $(Mg_{0.9375},Fe_{0.0625})SiO_3$, $(Mg_{0.8750},Fe_{0.1250})SiO_3$ and $(Mg_{0.9375},Fe_{0.0625})(Si_{0.9375},Fe_{0.0625})O_3$ are examined; charge substitution configuration plays essential role in the spin transition.

Table 3
List of recent studies on the spin states of iron in post-perovskite at high pressures

Composition	Fe^{3+} (%)	Method	Results	Reference
$(Mg,Fe)SiO_3$	0	Theory	No spin transition	Stackhouse et al. (2006)[a]
$Al–(Mg,Fe)SiO_3$	0, 100	Theory	No spin transition	Zhang and Oganov (2006)[b]
$(Mg_{0.9},Fe_{0.1})SiO_3$	~25	Emission	Low-spin Fe^{2+} and Fe^{3+} suggested	Badro et al. (2004)[c]

[a] Examined compositions are $(Mg_{0.9375},Fe_{0.0625})SiO_3$ and $(Mg_{0.875},Fe_{0.125})SiO_3$.
[b] Fe^{2+} in the high-spin state, Fe^{3+} in Mg site in the high-spin state, and Fe^{3+} in Si site in the low-spin state at the mantle pressures.
[c] Low-spin Fe^{2+} and Fe^{3+} in post-perovskite were suggested, but no structural confirmation for the existence of the post-perovskite phase was provided.

2004) (Table 3). On the other hand, *ab initio* simulations for the post-perovskite show that Fe^{3+} on the Mg site and all Fe^{2+} are in the high-spin state, while Fe^{3+} on the Si site is in the low-spin state (Stackhouse et al., 2006; Zhang and Oganov, 2006). Alternatively, theoretical calculations predicted a disproportionation of Fe^{2+} into metallic iron and Fe^{3+} in perovskite as well as in post-perovskite (Zhang and Oganov, 2006). However, the standard density functional theory (DFT) formalisms used in these studies for perovskite and post-perovskite, such as the LDA and generalized gradient approximation (GGA), are well-known to fail to reproduce many body effects, and thus relative energies, in the strongly correlated systems (e.g., Tsuchiya et al., 2006b). More sophisticated methods including internally consistent LDA + U are expected to provide much more reliable results for understanding the electronic spin and valence states of iron in perovskite and post-perovskite.

It is noteworthy to emphasize that X-ray emission spectroscopy probes the overall intensity of the Kβ emission line but does not necessarily differentiate individual contributions of the Fe^{2+} and Fe^{3+} species to the satellite intensity. Crystal-field theory with assumed site occupancies is thus used to interpret the X-ray emission spectra, though site occupancy of the Fe^{2+} and Fe^{3+} species in perovskite and post-perovskite remains poorly understood under high pressures (Badro et al., 2004; Li et al., 2004, 2006). Compared to the X-ray emission spectra of the high-spin and low-spin ferropericlase (Lin et al., 2005), Al-bearing perovskite still exhibits observable satellite peak intensity up to 100 GPa, and Al-free perovskite up to 145 GPa (Fig. 3). Furthermore, the position of the Kβ main peak, whose energy shift can be used as an additional line of evidence for the spin transition (Lin et al., 2006a, 2007b), is only shifted by 0.75–1.0 eV in silicate perovskite by pressures as high as 145 GPa, much less than that of ferropericlase (Fig. 2) (Badro et al., 2004; Li et al., 2004; Lin et al., 2005, 2007b). The residual intensity of the satellite peak and the lesser energy shift of the main Kβ peak indicate that the spin transition of iron in perovskite is likely incomplete or only occurs in one of the valence species in current high-pressure experimental results at 300 K. Some of the discrepancy discussed above likely arises from the use of the simplified crystal-field theory to interpret the experimental data for the complex crystal structure of perovskite and post-perovskite with multiple valence states and crystallographic sites, together with lattice distortion. Interpretation of these experimental data could be further complicated by the fact that silicate perovskite is known to be metastable under ambient conditions and tends to become amorphous under non-hydrostatic compression or excess heating, i.e., by intense irradiation of the laser beam or synchrotron X-ray (Dunben and Wolf, 1992; Gloter et al., 2000). Site occupancy and charge substitution mechanism all need to be understood to better address the spin and valence states of iron in perovskite and post-perovskite.

3. Effects of the spin transitions

The geophysical relevance of the electronic spin transition resides in its effects on the physical and chemical properties of the lower-mantle phases. Here we evaluate the consequences of spin transitions on properties of the lower-mantle phases, mainly in ferropericlase, because the reported transitions for perovskite and perhaps post-perovskite are still under debate and appear to be more complex than those in ferropericlase and their associated effects remain largely unknown.

3.1. Density, incompressibility, and sound velocities

Addition of FeO into MgO is well-known to increase the density and unit cell volume in the high-spin ferropericlase under ambient conditions (e.g., Jacobsen et al., 2002). The electronic spin-pairing transition, however, results in a smaller ionic radius of iron (Shannon and Prewitt, 1969) and thus a bulk volume reduction of 2–4% in ferropericlase containing 17–20% iron as seen in high-pressure X-ray diffraction studies (Lin et al., 2005; Speziale et al., 2005, 2007; Fei et al., 2007) and theoretical calculations (Tsuchiya et al., 2006a,b) (Figs. 4 and 5). The experimentally estimated effective ionic radius for the low-spin Fe^{2+} in ferropericlase is 0.70–0.72 Å (Fei et al., 2007). The volume reduction across the spin-pairing transition for an FeO_6 octahedron is about 8% in $(Mg_{0.8125},Fe_{0.1875})O$ in theoretical calculations (Tsuchiya et al., 2006a,b). The low-spin ferropericlase with various iron contents shows slightly smaller unit cell volume than that of pure MgO at pressures close to the spin transition (Lin et al., 2005; Fei et al., 2007), indicating that the low-spin FeO_6 octahedron is slightly smaller in size to the MgO_6 octahedron (Fig. 4). The spin transition thus enhances the compositional effect of the addition of FeO on the density of (Mg,Fe)O; the volume collapse of 2–4% across the spin transition is equivalent to 3–5% variation in iron content in ferropericlase (Figs. 4 and 5). Addition of FeO into MgO stabilizes the high-spin state to much higher pressures (Lin et al., 2006a; Fei et al., 2007).

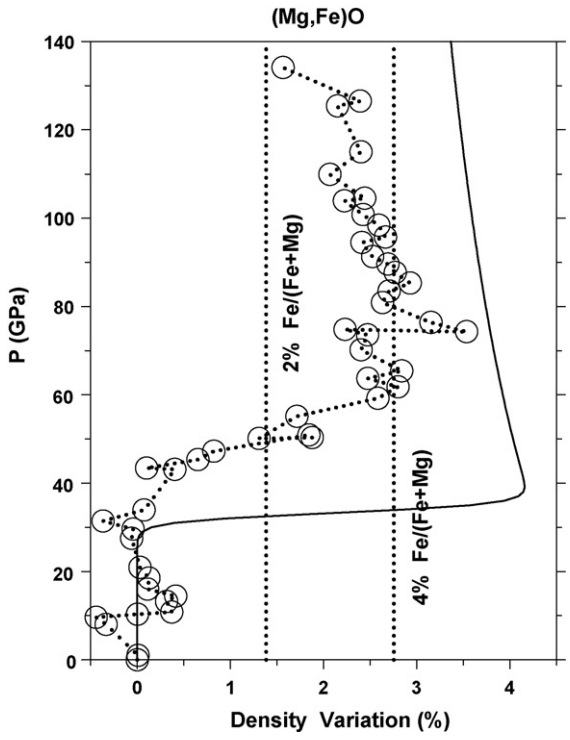

Fig. 5. Density variation across the electronic spin crossover in ferropericlase at high pressures. The percentage of the experimentally determined density variation is calculated using the density difference between the experimentally observed density (Lin et al., 2005) and the density of the high-spin state (see Fig. 4) divided by the extrapolated density of the high-spin state (open circles with dotted line). Open circles: $(Mg_{0.83},Fe_{0.17})O$ from Lin et al. (2005). Solid line: $(Mg_{0.8125},Fe_{0.1875})O$ from Tsuchiya et al. (2006a). Vertical dotted lines represent density variation of 1.4% and 2.8% by adding 2% and 4% FeO into MgO at ambient conditions, respectively (Jacobsen et al., 2002). Density variation for $(Mg_{0.83},Fe_{0.17})O$ is approximately 2.8% in X-ray experiments (Lin et al., 2005) and 4.2% for $(Mg_{0.8125},Fe_{0.1875})O$ in theoretical calculations (Tsuchiya et al., 2006a).

Since *a priori* knowledge of the ratio of the spin states is required to model the compression behavior, namely isothermal bulk modulus (K_T) and its pressure derivative (K'_T), of the high-spin and low-spin states, X-ray diffraction data should be used with recent Mössbauer and X-ray emission results with the known pressure range of the spin transition in order to better derive the equation of state (EoS) parameters for the high-spin and low-spin states (Lin et al., 2005, 2006a, 2007b,d) (Figs. 1 and 4). Alternatively, one can use the equation of state of the high-spin state, which is relatively well known, as a reference for deriving the volume and density variation of the compressed ferropericlase across the spin transition (Figs. 4 and 5). Results show that density of $(Mg_{0.83},Fe_{0.17})O$ starts to deviate from that of the high-spin $(Mg_{0.83},Fe_{0.17})O$ reference at ~43 GPa and reaches a maximum variation of ~2.8% at ~60 GPa in the X-ray diffraction data, consistent with the spin transition pressures observed in recent Mössbauer and X-ray emission studies (Figs. 1, 4 and 5) (Lin et al., 2006a, 2007b). Such analysis allows relatively reliable choice of the pressure range for evaluating the volume and incompressibility changes associated with the spin transition (Figs. 4 and 5). Based on these analyses, the K_{0T} for the low-spin ferropericlase derived from fitting the experimental data above 61 GPa (Lin et al., 2005; Figs. 4 and 5) is 205 (±16) GPa with V_{0LS}/V_{0HS} of 0.936 (±0.067) and an assumed K'_{0T} of 4, as compared to previously reported values of K_{0T} of 245 (±21) GPa with an assumed K'_{0T} of 4 and V_{0LS}/V_{0HS} of 0.904 (±0.016) (Lin et al., 2005). These analyses show that the bulk modulus increases by 6.3% and the bulk sound velocity increases by 1.5% across the high-spin to low-spin transition. The density increase of approximately 2.8% in $(Mg_{0.83},Fe_{0.17})O$ is equivalent to the effect of adding about 4% FeO into MgO (e.g., Jacobsen et al., 2002), whereas a density increase of about 4.2% is predicted in theoretical calculations (Tsuchiya et al., 2006a) (Fig. 5). A separate high-pressure study using laser annealing showed that the volume collapse across the spin transition is 1.8% in $(Mg_{0.8},Fe_{0.2})O$ and 3.1% in $(Mg_{0.61},Fe_{0.39})O$, respectively, indicating that the volume collapse is sensitive to the hydrostaticity of the sample, i.e., pressure medium and annealing process (Fei et al., 2007).

Evidence for the spin crossover may also lie in the shockwave data of ferropericlase as a continuous volume reduction of a few percent was observed in $(Mg_{0.6},Fe_{0.4})O$ and $(Mg_{0.9},Fe_{0.1})O$ at around 120 GPa (Vissiliou and Ahrens, 1982; Zhang and Gong, 2006).

The effect of the spin transition on the volume reduction of silicate perovskite and post-perovskite remains to be studied experimentally, though theoretical calculations show that the volume reduction is approximately 0.5% in silicate perovskite with a geophysically relevant composition (Stackhouse et al., 2007). Such smaller volume reduction is understandable because of the lesser amount of iron and likely gradual spin crossover behavior in perovskite.

The electronic spin-pairing transition of iron is also found to influence the sound velocities, and thermodynamic and vibrational properties of ferropericlase under high pressures and room temperatures (Lin et al., 2006b, 2007c; Crowhurst et al., 2008), but its effects on the properties of silicate perovskite are shown to be relatively small (Stackhouse et al., 2007). Compressional (V_p) and shear wave (V_s) velocities and their pressure derivatives rise dramatically across the spin transition of iron in $(Mg_{0.75}Fe_{0.25})O$ above 50 GPa (Lin et al., 2006b), and a reduction in sound velocities within the spin transition is also reported (Crowhurst et al., 2008). These effects of the spin transition on the incompressibility and sound velocities of (Mg,Fe)O at lower-mantle pressures are in contrast to what is predicted from studies of the pure MgO and high-spin ferropericlase. In particular, the effect of the spin transition on the sound velocities can partially affect the effect of the addition of iron in the lower-mantle minerals (Lin et al., 2006b), affecting the evaluation of the lower-mantle chemical heterogeneities.

3.2. Chemical behavior

The volume reduction and change in the electronic configuration across the spin transition of iron mentioned above may in turn affect the chemical behavior, namely the partition coefficient of iron, in the lower-mantle phases. Because of the difference in the effective ionic radius between the high-spin and low-spin octahedral Fe^{2+}, for example, iron would favorably

occupy the low-spin site with lower volume in order to minimize the Gibbs free energy of the system (Tsuchiya et al., 2006a). It is proposed that the spin transition would thus promote partitioning of iron into ferropericlase relative to perovskite and would result in a compositionally distinct layer with iron enriched in ferropericlase at depths below the mid-lower mantle (Badro et al., 2003, 2005); however, such conjecture is not supported by recent experimental studies which show that the partition coefficient of iron between ferropericlase and perovskite under lower-mantle conditions remains almost constant (Mao et al., 1997; Andrault, 2001; Kesson et al., 2002; Murakami et al., 2005; Kobayashi et al., 2005). We propose that the spin crossover with a continuous nature (Sturhahn et al., 2005; Tsuchiya et al., 2006a) readily explains why no significant change in iron partitioning between ferropericlase and perovskite occurs in a pyrolitic and olivine composition under lower-mantle pressure–temperature conditions. It is noteworthy that the basis for the thermodynamic calculations on the partition coefficient of iron between ferropericlase and perovskite (Badro et al., 2003, 2005) requires the knowledge on the energy changes associated with the spin transition which remain largely unknown, and calculated partition coefficient can vary by several orders of magnitude with changes in volume and spin-pairing energies (Badro et al., 2003, 2005), making this type of evaluation practically unreliable (Lin et al., 2005). In light of the observed effect of the spin transition on the volume reduction in ferropericlase, the use of the extrapolated unit cell parameters of ferropericlase and perovskite to determine the partition coefficient of iron between these phases at high pressures and temperatures (Mao et al., 1997) has become unreliable without the knowledge of the thermal equation of state with consideration of the spin crossover (Fig. 6).

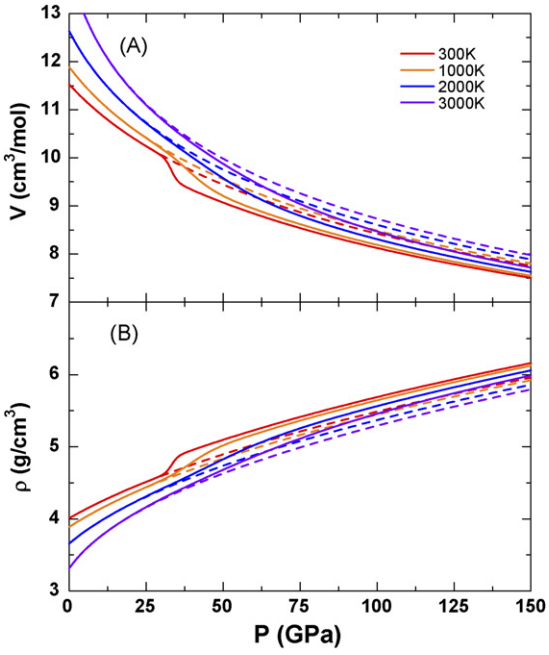

Fig. 6. Theoretically calculated molar volume (A) and density (B) profiles of $(Mg_{0.8125},Fe_{0.1875})O$ at high pressures and temperatures. The pressure–volume and pressure–density curves are calculated using the fractions of the high-spin to low-spin states at high pressures and temperatures by Tsuchiya et al. (2006a). Thermal compression parameters for the low-spin ferropericlase, namely thermal expansion coefficient and temperature derivative of the bulk modulus, are assumed to be similar to that of pure MgO (Fei, 1999; Karki et al., 2000; van Westrenen et al., 2005), because high-spin ferropericlase exhibits similar thermal expansion coefficient and pressure/temperature derivatives of the bulk modulus to that of pure MgO.

A significant change in the iron partitioning is reported to occur across the perovskite to post-perovskite phase transition (Murakami et al., 2005; Kobayashi et al., 2005; Sinmyo et al., 2006; Zhang and Oganov, 2006) and post-perovskite may accommodate very high proportions of Fe^{3+} with $Fe^{3+}/\Sigma Fe$ ratio on the order of 0.65 (Sinmyo et al., 2006); however, whether or not post-perovskite is enriched in iron relative to perovskite and how much more Fe^{3+} was introduced in the pressure-quench process of the sample are still under debate (Murakami et al., 2005; Kobayashi et al., 2005; Sinmyo et al., 2006). Experimental and theoretical evidence also shows decomposition of ferrous iron in perovskite and post-perovskite into metallic iron and ferric iron (Frost et al., 2004; Kobayashi et al., 2005; Zhang and Oganov, 2006).

It appears that for the low iron concentrations expected in the lower mantle the spin transition has a continuous nature, like a second-order transition, involving a mixed population of the high-spin and low-spin states (Tsuchiya et al., 2006a,b). Under certain circumstances, such as high iron concentration, it is still unclear if the spin transition would result in a binary loop; that is, the separation of two distinct phases with different compositions. This may have been suggested by some experiments (Dubrovinski et al., 2000) but not confirmed by others (Lin et al., 2003; Kondo et al., 2004).

3.3. Transport and rheological properties

Because of the partially filled 3d-electron orbitals that exhibit a band gap in the eV range, the presence of Fe strongly affects the radiative component of the thermal conduction (e.g., Burns, 1993) and the electrical conductivity (e.g., Dobson et al., 1997; Dobson and Brodholt, 2000; Lin et al., 2007c) of the mantle minerals. For example, the six 3d electrons of Fe^{2+} occupy the triplet t_{2g}-like orbitals in the low-spin ferropericlase which differ significantly in the electronic configurations from that of the high-spin ferropericlase (Tsuchiya et al., 2006a,b).

High-spin iron displays crystal-field absorption bands in the near-infrared range in oxides and silicates (e.g., Burns, 1993; Shen et al., 1994). Increasing iron concentration in the lower-mantle ferropericlase and silicate perovskite enhances optical absorption and hence reduces radiative thermal conductivity (e.g., Burns, 1993). The spin transition of iron in ferropericlase at approximately 60 GPa is reported to further enhance the optical absorption in the mid- and near-infrared spectral range, whereas the absorption edge at the ultraviolet region is reduced (Goncharov et al., 2006; Keppler et al., 2007). The spin-pairing transition is estimated to reduce the radiative thermal conductivity of ferropericlase by about 15% (Keppler et al., 2007) or more (Goncharov et al., 2006) at ~60 GPa and room temperature, and such effect may be further enhanced when other impurities and defects such as Fe^{3+} are present. Considering the spin crossover of iron with elevated lattice thermal conductiv-

ity under lower-mantle conditions, it remains to be seen if the effect of the spin transition on the radiative thermal conductivity would significantly affect the mode of the mantle convection in the lower mantle (Hofmeister, 1999; Matyska and Yuen, 2006; Naliboff and Kellogg, 2006). The absorption band in perovskite was reported to shift towards shorter wavelength (blue shift) as a result of the spin transition (Badro et al., 2004), as opposed to the red shift in ferropericlase (Tsuchiya et al., 2006a,b).

Electrical conductivity of the lower-mantle ferropericlase–$(Mg_{0.75},Fe_{0.25})O$ across the spin transition has been recently measured using designer diamond anvils to pressures over 1 Mbar and temperatures up to 500 K (Lin et al., 2007c). The electrical conductivity of $(Mg_{0.75},Fe_{0.25})O$ gradually rises by an order of magnitude up to 50 GPa but decreases by a factor of approximately 3 between 50 and 70 GPa. This decrease in the electrical conductivity is attributed to the isosymmetric high-spin to low-spin transition of iron in ferropericlase. That is, the electronic spin transition of iron results in a decrease in the mobility and/or density of the charge transfer carriers in the low-spin ferropericlase. The activation energy of the low-spin ferropericlase is 0.27 eV at 101 GPa, consistent with the small polaron conduction (electronic hopping, charge transfer). An extrapolation of the electrical conductivity of the low-spin ferropericlase to the lower-mantle pressure–temperature conditions (~2500 K and ~100 GPa) yields an electrical conductivity in the order of tens of S/m (Lin et al., 2007c), consistent with the model values for the lower mantle (e.g., Olsen, 1999); though, the electrical conductivity mechanism of ferropericlase at the lower-mantle pressure–temperature conditions remains to be studied because a large polaron mechanism is suggested to be dominant at lower-mantle temperatures (Dobson et al., 1997).

Other effects of the spin transition on the elastic anisotropy, viscosity, diffusivity, and rheology, including lattice preferred orientation, stress field, and plasticity, of the lower-mantle phases all remain to be understood. In particular, the relatively low creep strength and large elastic anisotropy of ferropericlase, as the second most dominant constituent of the Earth's lower mantle, are believed to play very important roles in the viscosity, dynamics, and seismic anisotropy of the lower mantle (Karato, 1989; Forte and Mitrovica, 2001; Yamazaki and Karato, 2002; Long et al., 2006). Recent high-pressure results already showed that the low-spin ferropericlase is stiffer and has higher shear modulus than the high-spin ferropericlase (Lin et al., 2005, 2006b). Such changes may indicate that the viscosity and rheology of the low-spin ferropericlase likely differs from that of the high-spin ferropericlase.

4. Geophysical implications and conclusions

To understand the geophysical consequences of the spin transition in the lower mantle, we have modeled the density and bulk modulus profiles of ferropericlase with and without considering the effect of the spin transition (Figs. 6–9). As the spin crossover of iron occurs in the lower-mantle minerals such as ferropericlase at high pressures and temperatures, their thermal compression curves and sound velocities will be continuously influenced by the ratio of the high-spin and low-spin states along the lower-mantle geotherm (Figs. 3 and 4). Because high-spin ferropericlase shows similar thermal compression behavior to that of pure MgO (Fei, 1999; Wentzcovitch et al., 2004), we assume that low-spin ferropericlase with various iron contents also exhibits similar behavior in our calculations. Using the spin crossover model of $(Mg_{0.8125},Fe_{0.1875})O$ (Tsuchiya et al., 2006a)

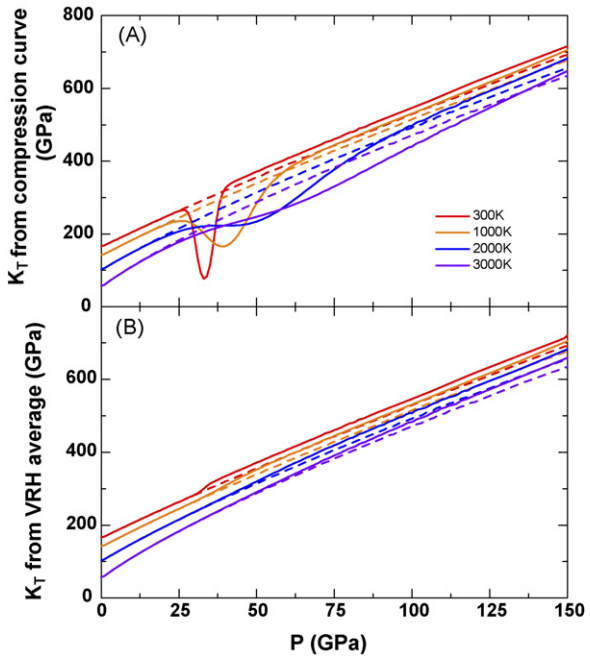

Fig. 7. Calculated isothermal bulk modulus (K_T) of $(Mg_{0.8125},Fe_{0.1875})O$ at high pressures and temperatures: (A) calculated bulk modulus using the pressure derivative of volume ($-V\mathrm{d}P/\mathrm{d}V$) along the pressure–volume curves in Fig. 5; (B) calculated bulk modulus using the Voigt–Ruess–Hill (VRH) average model with the fraction of the high-spin/low-spin states and their bulk moduli (Tsuchiya et al., 2006a). Solid lines: spin crossover model; dashed lines: high-spin state only.

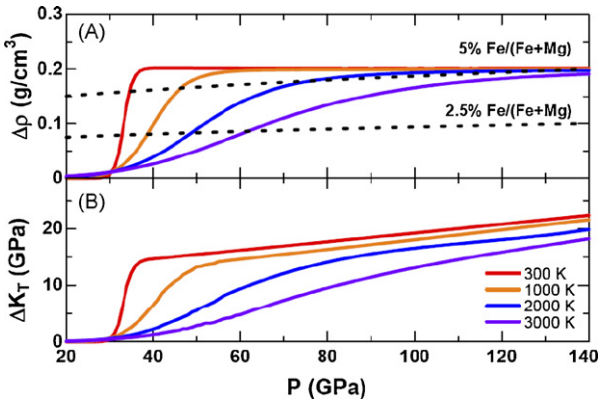

Fig. 8. Calculated density (A) and bulk modulus (B) differences for $(Mg_{0.8125},Fe_{0.1875})O$. The differences are calculated using the spin crossover model at 300, 1000, 2000 and 3000 K (same colors in Fig. 6) (Tsuchiya et al., 2006a) as compared with that without the spin crossover (Figs. 6 and 7). Dotted lines represent density variation produced by adding 2% and 5% FeO into MgO at 300 K. The density variation by considering the spin crossover is about 0.19 g/cm^3 (±3.5%) at 2000 K and 100 GPa which is equivalent to adding 5.0% FeO into MgO. Bulk modulus variation is estimated within the model shown in Fig. 7(B).

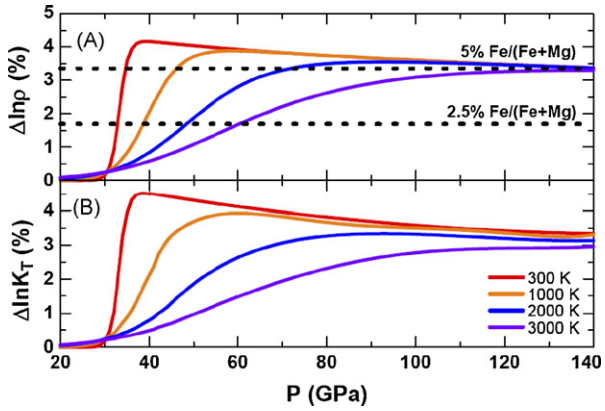

Fig. 9. Calculated density (A) and bulk modulus (B) variations in percentage for $(Mg_{0.8125},Fe_{0.1875})O$ as derived from Fig. 8.

and the quasiharmonic *ab initio* thermodynamics described by Karki et al. (2000), a sharp density contrast of ~4.2% can be seen in $(Mg_{0.8125},Fe_{0.1875})O$ across the spin transition at room temperature (Fig. 5) but the contrast becomes continuous due to the spin crossover at temperatures above 1000 K (Figs. 6, 8 and 9). Such density increase is equivalent to the addition of ~5.0% FeO into MgO in ferropericlase (Figs. 8 and 9). Along the lower-mantle geotherm (Brown and Shankland, 1981), the spin crossover in ferropericlase and perhaps in perovskite would lead to an increasingly steeper than normal density gradient as compared to that without the spin crossover (Figs. 6, 8 and 9). For a pyrolite composition with approximately 33% ferropericlase and 67% aluminous silicate perovskite (Ringwood, 1982), the increase in density induced by the spin crossover in ferropericlase could be approximately 1% toward the bottom of the lower mantle.

Here we also evaluate the effect of the spin transition on the bulk modulus of ferropericlase under high pressures and temperatures. Bulk modulus (K) is, by thermodynamic definition:

$$K = -V\frac{dP}{dV} = -\frac{dP}{d\ln V} \quad (1)$$

where P is pressure and V is volume. Since the spin crossover of iron results in a continuous volume reduction in ferropericlase at high pressures and temperatures (Fig. 6), a classical equation of state using finite stress–strain theory (Birch, 1986; Davies and Dziewonski, 1975) is thus unreliable for deriving the bulk modulus and its pressure derivative (K') from the pressure–volume curve without knowing the ratio of the spin states (n). To signify this issue, we have derived the isothermal bulk modulus of ferropericlase from theoretically calculated pressure–volume curves using Eq. (1) (Fig. 7A). Results show that softening in the bulk modulus is very significant in the spin transition at room temperature but is reduced across the spin crossover at high temperatures. The physical meaning of this behavior remains to be further understood, because the volume variation also includes a contribution from successive volume reductions associated with the spin crossover. Theoretical calculations show that ferropericlase with a fixed composition and ratio of the high-spin to low-spin states can be defined as having its own compression curve, and increasing the low-spin state component with increasing pressure slightly increases its bulk modulus of (Tsuchiya et al., 2006a). That is, the pressure–volume relation across the spin crossover may not be treated as a compression curve of a single state. Since individual theoretical calculations of the bulk modulus with fine-scale ratios of the spin states would be extremely time consuming, here we have simply derived the bulk modulus of the mixed spin states from a Voigt–Ruess–Hill (VRH) average model. Results from these calculations are generally in line with first principles calculations (Tsuchiya et al., 2006a) in which the bulk modulus monotonically increases with increasing pressure across the spin transition (Fig. 7B). In this case, the spin crossover introduces a density increase of ~0.2 g/cm^3 (~3%) and bulk modulus increase of ~20 GPa (~3%) in ferropericlase toward the lowermost mantle (Figs. 8 and 9). As the isothermal bulk modulus is typically derived from the thermal compression curves experimentally, these two models here point to the need to measure the bulk modulus as well as sound velocities directly in the spin crossover in order to better understand its behavior. Uncertainties such as the exact fraction of the high-spin and low-spin states and its influence on the thermal equation of state of the lower-mantle minerals remain to be better understood to refine the density and bulk modulus profiles in our calculations. It is possible that the low-spin ferropericlase may exhibit a relatively lower thermal expansion coefficient due to its stiffer lattice, indicating stronger effects of the spin transition on the density and bulk modulus.

It is conceivable that sound velocities in ferropericlase at high pressures and temperatures would gradually deviate from that of the extrapolated high-spin state by increasing the fraction of the low-spin state. Therefore, the increase in the fraction of the low-spin ferropericlase may result in abnormal sound velocity gradients at the lower mantle conditions (e.g., van der Hilst and Kárason, 1999; Kellogg et al., 1999; Lin et al., 2006b; Crowhurst et al., 2008). Knowledge of the ratio of the high-spin to low-spin states in the lower-mantle phases, in particular in ferropericlase, as well as the effects of the spin transitions are thus needed to reliably evaluate the density, sound velocities, and transport properties of the Earth's lower mantle.

Owing to the dominant abundance of the silicate perovskite in the Earth's lower mantle and post-perovskite in the lowermost mantle, future *in situ* experimental measurements of the spin and valence states of iron and their associated effects on the physical properties is thus essential to address their effects on the geophysics and geochemistry of the Earth's lower mantle. In particular, the temperature effect on the spin and valence states of silicate perovskite and post-perovskite remains to be studied. Multidisciplinary approaches including theoretical calculations and employment of multiple experimental techniques are needed to uncover these unsettled issues.

Acknowledgements

We thank M.J. Lipps, V. Iota, and A. Lazicki for discussions. We also thank S. Speziale and W.A. Bassett for constructive comments. This work at LLNL was performed under the auspices of the U.S. DOE by University of California and LLNL

under Contract No. W-7405-Eng-48. JFL was also supported by Lawrence Livermore Fellowship. TT is supported by the Ehime University Project Fund and Grant-in-Aid for Scientific Research from the Japan Society for the Promotion of Science (nos. 18840033 and 19740331). Part of the study was completed during JFL's visit to GRC, Ehime University.

References

Andrault, D., 2001. Evaluation of (Mg, Fe) partitioning between silicate perovskite and magnesiowüstite up to 120 GPa and 2300 K. J. Geophys. Res. 106, 2079–2087.

Badro, J., Fiquet, G., Struzhkin, V.V., Somayazulu, M., Mao, H.K., Shen, G., Le Bihan, T., 2002. Nature of the high-pressure transition in Fe_2O_3 hematite. Phys. Rev. Lett. 89, 205504.

Badro, J., Fiquet, G., Guyot, F., Rueff, J.P., Struzhkin, V.V., Vankó, G., Monaco, G., 2003. Iron partitioning in Earth's mantle: toward a deep lower mantle discontinuity. Science 300, 789–791.

Badro, J., Rueff, J.P., Vankó, G., Monaco, G., Fiquet, G., Guyot, F., 2004. Electronic transitions in perovskite: possible nonconvecting layers in the lower mantle. Science 305, 383–386.

Badro, J., Fiquet, G., Guyot, F., 2005. Thermochemical state of the lower mantle: new insights from mineral physics. In: van der Hilst, R.D., Bass, J., Matas, J., Trampert, J. (Eds.), Earth's Deep Mantle: Structure, Composition, and Evolution. American Geophysical Union Monograph Series 160, Washington, DC, pp. 241–260.

Birch, F., 1986. Equation of state and thermodynamic parameters of NaCl to 300 kbar in the high-temperature domain. J. Geophys. Res. 91, 4949–4954.

Brown, J.M., Shankland, T.J., 1981. Thermodynamic parameters in the Earth as determined from seismic profiles. Geophys. J. R. Astron. Soc. 66, 579–596.

Burns, R.G., 1993. Mineralogical Applications of Crystal Field Theory. Cambridge University Press, Cambridge.

Cococcioni, M., de Gironcoli, S., 2005. Linear response approach to the calculation of the effective interaction parameters in the LDA + U method. Phys. Rev. B 71, 035105.

Cohen, R.E., Mazin, I.I., Isaak, D.G., 1997. Magnetic collapse in transition metal oxides at high pressure: implications for the Earth. Science 275, 654–657.

Crowhurst, J., Brown, J.M., Goncharov, A., Jacobsen, S.D., 2008. Elasticity of (Mg,Fe)O through the spin transition of iron in the lower mantle. Science 319, 451–453.

Davies, G.F., Dziewonski, A.M., 1975. Homogeneity and constitution of the Earth's lower mantle and outer core. Phys. Earth Planet. Inter. 10, 336–343.

Dobson, D.P., Richmond, N.C., Brodholt, J.P., 1997. A high-temperature electrical conduction mechanism in the lower mantle phase $(Mg, Fe)_{1-X}O$. Science 275, 1779–1781.

Dobson, D.P., Brodholt, J.P., 2000. The electrical conductivity of the lower mantle phase magnesiowüstite at high temperatures and pressures. J. Geophys. Res. 105, 531–538.

Dubrovinski, L.S., Dubrovinskaia, N.A., Saxena, S.K., Annersten, H., Hålenius, H., Harryson, H., Tutti, F., Rechi, S., Le Bihan, T., 2000. Stability of ferropericlase in the lower mantle. Science 289, 430–432.

Dunben, D.J., Wolf, G.H., 1992. High-temperature behavior of metastable $MgSiO_3$ perovskite: a Raman spectroscopic study. Am. Miner. 77, 890–893.

Dziewonski, A.M., Anderson, D.L., 1981. Preliminary reference Earth model. Phys. Earth Planet. Inter. 25, 297–356.

Fei, Y., 1999. Effects of temperature and composition on the bulk modulus of (Mg, Fe)O. Am. Miner. 84, 272–276.

Fei, Y., Zhang, L., Corgne, A., Watson, H.C., Ricolleau, A., Meng, Y., Prakapenka, V.B., 2007. Spin transition and equations of state of (Mg, Fe)O solid solutions. Geophys. Res. Lett. 34, L17307, doi:10.1029/2007GL030712.

Forte, A.M., Mitrovica, J.X., 2001. Deep-mantle high-viscosity flow and thermochemical structure inferred from seismic and geodynamic data. Nature 410, 1049–1056.

Frost, D.J., Liebske, C., Langenhorst, F., McCammon, C.A., Trønnes, R.G., Rubie, D.C., 2004. Experimental evidence for the existence of iron-rich metal in the Earth's lower mantle. Nature 428, 409–412.

Fyfe, W.S., 1960. The possibility of d-electron uncoupling in olivine at high pressures. Geochim. Cosmochim. Acta 19, 141–143.

Gaffney, E.S., Anderson, D.L., 1973. Effect of low-spin Fe^{2+} on the composition of the lower mantle. J. Geophys. Res. 78, 7005–7014.

Gavriliuk, A.G., Lin, J.F., Lyubutin, I.S., Struzhkin, V.V., 2006. Optimization of the conditions of synchrotron Mössbauer experiment for studying electron transitions at high pressures by the example of (Mg Fe)O magnesiowustite. J. Exp. Theor. Phys. Lett. 84, 161–166.

Gloter, A., Guyot, F., Martinez, I., Colliex, C., 2000. Electron energy-loss spectroscopy of silicate perovskite–magnesiowüstite high pressure assemblages. Am. Miner. 85, 1452–1458.

Goncharov, A.F., Struzhkin, V.V., Jacobsen, S.D., 2006. Reduced radiative conductivity of low-spin (Mg, Fe)O in the lower mantle. Science 312, 1205–1208.

Hofmeister, A.M., 1999. Mantle values of thermal conductivity and the geotherm from phonon lifetime. Science 283, 1699–1706.

Hofmeister, A.M., 2006. Is low-spin Fe^{2+} present in Earth's mantle? Earth Planet. Sci. Lett. 243, 44–52.

Jacobsen, S.D., Reichmann, H.J., Spetzler, H., Mackwell, S.J., Smyth, J.R., Angel, R.J., McCammon, C.A., 2002. Structure and elasticity of single-crystal (Mg, Fe)O and a new method of generating shear waves for gigahertz ultrasonic interferometry. J. Geophys. Res. 107 (B2), doi:10.1029/2001JB000490.

Jackson, J.M., Sturhahn, W., Shen, G., Zhao, J., Hu, M.Y., Errandonea, D., Bass, J.D., Fei, Y., 2005. A synchrotron Mössbauer spectroscopy study of (Mg, Fe)SiO_3 perovskite up to 120 GPa. Am. Miner. 90, 199–205.

Karato, S.I., 1989. Plasticity-crystal structure systematics in dense oxides and its implications for the creep strength of the Earth's deep interior: a preliminary result. Phys. Earth Planet. Inter. 55, 234–240.

Kantor, I.Yu., Dubrovinsky, L.S., McCammon, C.A., 2006. Spin crossover in (Mg, F)O: a Mössbauer effect study with an alternative interpretation of X-ray emission spectroscopy data. Phys. Rev. B 73, 100101.

Kantor, I.Yu., Dubrovinsky, L.S., McCammon, C.A., 2007. Reply to "comment on 'spin crossover in (Mg, F)O: a Mössbauer effect study with an alternative interpretation of X-ray emission spectroscopy data'". Phys. Rev. B 75, 177103.

Karki, B.B., Wentzcovitch, R.M., de Gironcoli, S., Baroni, S., 2000. *Ab initio* lattice dynamics of $MgSiO_3$ perovskite at high pressure. Phys. Rev. B 62, 14750–14756.

Kellogg, L.H., Hager, B.H., van der Hilst, R.D., 1999. Compositional stratification in the deep mantle. Science 283, 1881–1884.

Keppler, H., Kantor, I., Dubrovinsky, L.S., 2007. Optical absorption spectra of ferropericlase to 84 GPa. Am. Miner. 92, 433–436.

Kesson, S.E., Fitz Gerald, J.D., O'Neill, H.St.C., Shelley, J.M.G., 2002. Partitioning of iron between magnesian silicate perovskite and magnesiowüstite at about 1 Mbar. Phys. Earth Planet. Inter. 131, 295–310.

Kobayashi, Y., Kondo, T., Ohtani, E., Hirao, N., Miyajima, N., Yagi, T., Nagase, T., Kikegawa, T., 2005. Fe–Mg partitioning between (Mg,Fe)SiO_3 post-perovskite, perovskite, and magnesiowüstite in the Earth's lower mantle. Geophys. Res. Lett. 32, L19301, doi:10.1029/2005GL023257.

Kondo, T., Ohtani, E., Hirao, N., Yagi, T., Kikegawa, T., 2004. Phase transition of (Mg, Fe)O at high pressures. Phys. Earth Planet. Inter. 143–144, 201–213.

Li, J., Struzhkin, V.V., Mao, H.K., Shu, J., Hemley, R.J., Fei, Y., Mysen, B., Dera, P., Prakapenka, V., Shen, G., 2004. Electronic spin state of iron in lower mantle perovskite. Proc. Natl. Acad. Sci. U.S.A. 101, 14027–14030.

Li, J., Sturhahn, W., Jackson, J.M., Struzhkin, V.V., Lin, J.F., Zhao, J., Mao, H.K., Shen, G., 2006. Pressure effect on the electronic structure of iron in (Mg,Fe)(Al, Si)O_3 perovskite: a combined synchrotron Mössbauer and X-ray emission spectroscopy study up to 100 GPa. Phys. Chem. Miner. 33, 575–585.

Li, L., Brodholt, J.P., Stackhouse, S., Weidner, D.J., Alfredsson, M., Price, G.D., 2005. Electronic spin state of ferric iron in Al-bearing perovskite in the lower mantle. Geophys. Res. Lett. 32, L17307.

Lin, J.F., Heinz, D.L., Mao, H.K., Hemley, R.J., Devine, J.D., Li, J., Shen, G., 2003. Stability of magnesiowüstite in the Earth's lower mantle. Proc. Natl. Acad. Sci. 100, 4405–4408.

Lin, J.F., Struzhkin, V.V., Jacobsen, S.D., Hu, M., Chow, P., Kung, J., Liu, H., Mao, H.K., Hemley, R.J., 2005. Spin transition of iron in magnesiowüstite in Earth's lower mantle. Nature 436, 377–380.

Lin, J.F., Gavriliuk, A.G., Struzhkin, V.V., Jacobsen, S.D., Sturhahn, W., Hu, M., Chow, P., Yoo, C.S., 2006a. Pressure-induced electronic spin transition of iron in magnesiowüstite-(Mg, Fe)O. Phys. Rev. B 73, 113107.

Lin, J.F., Jacobsen, S.D., Sturhahn, W., Jackson, J.M., Zhao, J., Yoo, C.S., 2006b. Sound velocities of ferropericlase in Earth's lower mantle. Geophys. Res. Lett. 33, L22304, doi:10.1029/2006GL028099.

Lin, J.F., Jacobsen, S.D., Wentzcovitch, R.M., 2007a. Electronic spin transition of iron in the Earth's deep mantle. Eos. Trans. Am. Geophys. Union 88 (2), 13, 17.

Lin, J.F., Struzhkin, V.V., Gavriliuk, A.G., Lyubutin, I., 2007b. Comment on "Spin crossover in (Mg, Fe)O: a Mössbauer effect study with an alternative interpretation of X-ray emission spectroscopy data". Phys. Rev. B 75, 177102.

Lin, J.F., Weir, S.T., Jackson, D.D., Evans, W.J., Yoo, C.S., 2007c. Electrical conductivity of the low-spin ferropericlase in the Earth's lower mantle. Geophys. Res. Lett. 34, L16305, doi:10.1029/2007GL030523.

Lin, J.F., Vankó, G., Jacobsen, S.D., Iota-Herbei, V., Struzhkin, V.V., Prakapenka, V.B., Kuznetsov, A., Yoo, C.S., 2007d. Spin transition zone in Earth's lower mantle. Science 317, 1740–1743.

Lin, J.F., Jacobsen, S.D., Sturhahn, W., Jackson, J.M., Zhao, J., Yoo, C.S., 2007e. Correction to "Sound velocities of ferropericlase in Earth's lower mantle". Geophys. Res. Lett. 34, L09301, doi:10.1029/2007GL029880.

Long, M.D., Xiao, X., Jiang, Z., Evans, B., Karato, S.I., 2006. Lattice preferred orientation in deformed polycrystalline (Mg, Fe)O and implications for seismic anisotropy in D″. Phys. Earth Planet. Inter. 156, 75–88.

Mao, H.K., Shen, G., Hemley, R.J., 1997. Multivariable dependence of Fe–Mg partitioning in the lower mantle. Science 278, 2098–2100.

Mattern, E., Matas, J., Ricard, Y., Bass, J.D., 2005. Lower mantle composition and temperature from mineral physics and thermodynamic modeling. Geophys. J. Int. 160, 973–990.

Matyska, C., Yuen, D.A., 2006. Lower mantle dynamics with the post-perovskite phase change, radiative thermal conductivity, temperature- and depth-dependent viscosity. Earth Planet. Sci. Lett. 154, 196–207.

McCammon, C., 1997. Perovskite as a possible sink for ferric iron in the lower mantle. Nature 387, 694–696.

McCammon, C., 2006. Microscopic properties to macroscopic behavior: the influence of iron electronic states. J. Miner. Petrol. Sci. 101, 130–144.

Murakami, M., Hirose, K., Kawamura, K., Sata, N., Ohishi, Y., 2004. Post-perovskite phase transition in $MgSiO_3$. Science 304, 855–858.

Murakami, M., Hirose, K., Sata, N., Ohishi, Y., 2005. Post-perovskite phase transition and mineral chemistry in the pyrolitic lowermost mantle. Geophys. Res. Lett. 32, L03304.

Naliboff, J.B., Kellogg, L.H., 2006. Dynamical effects of a step-wise increase in thermal conductivity and viscosity in the lowermost mantle. Geophys. Res. Lett. 33, L12S09.

Oganov, A.R., Ono, S., 2004. Theoretical and experimental evidence for a post-perovskite phase of $MgSiO_3$ in Earth's D″ layer. Nature 430, 445–448.

Ohnishi, S., 1978. A theory of the pressure-induced high-spin–low-spin transition of transition metal oxides. Phys. Earth Planet. Inter. 17, 13–139.

Olsen, N., 1999. Long-period (30 days-1 year) electromagnetic sounding and the electrical conductivity of the lower mantle beneath Europe. Geophys. J. Int. 138, 179–187.

Persson, K., Bengtson, A., Ceder, G., Morgan, D., 2006. *Ab initio* study of the composition dependence of the pressure-induced spin transition in the $(Mg_{1-x}Fe_x)O$ system. Geophys. Res. Lett. 33, L16306.

Ringwood, A.E., 1982. Phase transformations and differentiation in subducted lithosphere: implications for mantle dynamics basalt petrogenesis and crustal evolution. J. Geol. 90, 611–642.

Shannon, R.D., Prewitt, C.T., 1969. Effective ionic radii in oxides and fluorides. Acta Crystallogr. B 25, 925–946.

Shen, G., Fei, Y., Hålenius, Wang, Y., 1994. Optical absorption spectra of (Mg, Fe)SiO_3 silicate perovskite. Phys. Chem. Miner. 20, 478–482.

Sherman, D.M., 1988. High-spin to low-spin transition of iron(II) oxides at high pressures: possible effects on the physics and chemistry of the lower mantle. In: Ghose, S., Coey, J.M.D., Salje, E. (Eds.), Structural and Magnetic Phase Transitions in Minerals. Springer-Verlag, New York, pp. 113–118.

Sherman, D.M., 1991. The high-pressure electronic structure of magnesiowüstite (Mg, Fe)O: applications to the physics and chemistry of the lower mantle. J. Geophys. Res. 96 (B9), 14299–14312.

Sherman, D.M., Jansen, H.J.F., 1995. First-principles predictions of the high-pressure phase transition and electronic structure of FeO: implications for the chemistry of the lower mantle and core. Geophys. Res. Lett. 22, 1001–1004.

Speziale, S., Zha, C.-S., Duffy, T.S., Hemley, R.J., Mao, H.K., 2001. Quasi-hydrostatic compression of magnesium oxide to 52 GPa: implications for the pressure–volume–temperature equation of state. J. Geophys. Res. 106, 515–528.

Speziale, S., Milner, A., Lee, V.E., Clark, S.M., Pasternak, M., Jeanloz, R., 2005. Iron spin transition in Earth's mantle. Proc. Natl. Acad. Sci. 102, 17918–17922.

Speziale, S., Lee, V.E., Clark, S.M., Lin, J.F., Pasternak, M.P., Jeanloz, R., 2007. Effects of Fe spin transition on the elasticity of (Mg, Fe)O magnesiowüstites and implications for the seismological properties of the Earth's lower mantle. J. Geophys. Res. 112, B10212, doi:10.1029/2006JB004730.

Stackhouse, S., Brodholt, J.P., Dobson, D.P., Price, G.D., 2006. Electronic spin transitions and the seismic properties of ferrous iron bearing $MgSiO_3$ post-perovskite. Geophys. Res. Lett. 33, L12S03.

Stackhouse, S., Brodholt, J.P., Price, G.D., 2007. Electronic spin transitions in iron-bearing $MgSiO_3$ perovskite. Earth Planet. Sci. Lett. 253, 282–290.

Sturhahn, W., Jackson, J.M., Lin, J.F., 2005. The spin state of iron in Earth's lower mantle minerals. Geophys. Res. Lett. 32, L12307.

Sinmyo, R., Hirose, K., O'Neill, H.St.C., Okunishi, E., 2006. Ferric iron in Al-bearing post-perovskite. Geophys. Res. Lett. 33, L12S13.

Trampert, J., Deschamps, F., Resovsky, J., Yuen, D., 2004. Probabilistic tomography maps chemical heterogeneities throughout the lower mantle. Science 306, 853–856.

Tsuchiya, T., Tsuchiya, J., Umemoto, K., Wentzcovitch, R.M., 2004. Phase transition in $MgSiO_3$ perovskite in the Earth's lower mantle. Earth Planet. Sci. Lett. 224, 241–248.

Tsuchiya, T., Wentzcovitch, R.M., da Silva, C.R.S., de Gironcoli, S., 2006a. Spin transition in magnesiowüstite in Earth's lower mantle. Phys. Rev. Lett. 96, 198501.

Tsuchiya, T., Wentzcovitch, R.M., da Silva, C.R.S., de Gironcoli, S., Tsuchiya, J., 2006b. Pressure induced high spin to low spin transition in magnesiowüstite. Phys. Stat. Sol. (b) 243, 2111–2116.

van der Hilst, R.D., Kárason, H., 1999. Compositional heterogeneity in the bottom 1000 kilometers of Earth's mantle: toward a hybrid convection model. Science 283, 1885–1888.

van Westrenen, W., Li, J., Fei, Y., Frank, M.R., Hellwig, H., Komabayashi, T., Mibe, K., Minarik, W.G., Van Ormanh, J.A., Watson, H.C., Funakoshi, K.I., Schmidt, M.W., 2005. Thermoelastic properties of $(Mg_{0.64}Fe_{0.36})O$ ferropericlase based on in situ X-ray diffraction to 26.7 GPa and 2173 K. Phys. Earth Planet. Inter. 151, 163–176.

Vankó, G., Neisius, T., Molnár, G., Renz, F., Kárpáti, S., Shukla, A., de Groot, F.M.F., 2006. Probing the 3d spin momentum with X-ray emission spectroscopy: the case of molecular-spin transitions. J. Phys. Chem. B 110, 11647–11653.

Vankó, G., de Groot, F., 2007. Comment on "Spin crossover in (Mg, Fe)O: a Mössbauer effect study with alternative interpretation of X-ray emission spectroscopy data". Phys. Rev. B 75, 177101.

Vissiliou, M.S., Ahrens, T.J., 1982. The equation of state of $Mg_{0.6}Fe_{0.4}O$ to 200 GPa. Geophys. Res. Lett. 9, 127–130.

Wentzcovitch, R.M., Karki, B.B., Cococcioni, M., de Gironcoli, S., 2004. Thermoelastic properties of $MgSiO_3$-perovskite: insights on the nature of the Earth's lower mantle. Phys. Rev. Lett. 92, 018501.

Yamazaki, D., Karato, S.I., 2002. Fabric development in (Mg,Fe)O during large strain, shear deformation: implications for seismic anisotropy in Earth's lower mantle. Phys. Earth Planet. Inter. 131, 251–267.

Zhang, F., Oganov, A.R., 2006. Valence state and spin transitions of iron in Earth's mantle silicates. Earth Planet. Sci. Lett. 249, 436–443.

Zhang, L., Gong, Z.Z., 2006. Shock compression and phase transitions of magnesiowustite (Mg, Fe)O up to Earth's lowermost mantle conditions. Chin. Phys. Lett. 23, 3049–3051.